Land use/land cover and scale influences on in-stream nitrogen uptake kinetics

Tim Covino,[1] Brian McGlynn,[1] and Rebecca McNamara[1,2]

Received 29 September 2011; revised 10 February 2012; accepted 18 February 2012; published 17 April 2012.

[1] Land use/land cover change often leads to increased nutrient loading to streams; however, its influence on stream ecosystem nutrient transport remains poorly understood. Given the deleterious impacts elevated nutrient loading can have on aquatic ecosystems, it is imperative to improve understanding of nutrient retention capacities across stream scales and watershed development gradients. We performed 17 nutrient addition experiments on six streams across the West Fork Gallatin Watershed, Montana, USA, to quantify nitrogen uptake kinetics and retention dynamics across stream sizes (first to fourth order) and along a watershed development gradient. We observed that stream nitrogen (N) uptake kinetics and spiraling parameters varied across streams of different development intensity and scale. In more developed watersheds we observed a fertilization affect. This fertilization affect was evident as increased ash-free dry mass, chlorophyll *a*, and ambient and maximum uptake rates in developed as compared to undeveloped streams. Ash-free dry mass, chlorophyll *a*, and the number of structures in a subwatershed were significantly correlated to nutrient spiraling and kinetic parameters, while ambient and average annual N concentrations were not. Additionally, increased maximum uptake capacities in developed streams contributed to low in-stream nutrient concentrations during the growing season, and helped maintain watershed export at low levels during base flow. Our results indicate that land use/land cover change can enhance in-stream uptake of limiting nutrients and highlight the need for improved understanding of the watershed dynamics that control nutrient export across scales and development intensities for mitigation and protection of aquatic ecosystems.

Citation: Covino, T., B. McGlynn, and R. McNamara (2012), Land use/land cover and scale influences on in-stream nitrogen uptake kinetics, *J. Geophys. Res.*, *117*, G02006, doi:10.1029/2011JG001874.

1. Introduction

[2] Land use and land cover change is occurring at increasing rates across the western United States. Historically, land use in the region was primarily extractive (e.g., mining, logging, agriculture); however, over the last few decades, tourism, recreation, and mountain/resort development have increased. These recent shifts in land use and land cover have elevated nutrient loading to many streams across the region, relative to nutrient loads prior to development [e.g., *Biggs et al.*, 2004; *Mueller and Spahr*, 2006; *Whitehead et al.*, 2002]. Nutrients, such as nitrogen (N) and phosphorus (P), are essential to stream biotic activity [*Mulholland and Webster*, 2010] and often limit ecosystem productivity [*Vitousek and Howarth*, 1991]. In many streams of the western United States, N can limit productivity [e.g., *Grimm and Fisher*, 1986], and excess N loading can have deleterious impacts on water quality and ecosystem function (e.g., eutrophication). Nutrient concentrations and/or loads in excess of biotic demand indicate saturation relative to the nutrient of concern. In addition to impacting aquatic ecosystems locally, excess nutrients can also be exported downstream, which can lead to degradation of coastal estuaries and eutrophication of marine environments [*Rabalais et al.*, 2010]. Therefore elevated nutrient loading can have potentially negative impacts on both local and downstream communities due to the linked nature of fluvial ecosystems.

[3] Increased nutrient loading to streams can affect watershed nutrient retention capacities and export magnitudes. While considerable research has focused on nutrient cycling and retention in first and second order streams [*Ensign and Doyle*, 2006], the influence these dynamics exert over downstream export and loading to receiving water bodies remains poorly understood (but see *Peterson et al.* [2001]). Stream uptake kinetics are not well understood because very few studies have quantified these dynamics across concentration ranges. Additionally, it is not well known how nutrient uptake varies at the watershed or stream network scale or how uptake kinetics differ within watersheds that have varying development intensities and associated nutrient loading magnitudes. Understanding and predicting the fate and export of N requires quantification of

[1]Department of Land Resources and Environmental Sciences, Montana State University, Bozeman, Montana, USA.
[2]United States Forest Service, Butte, Montana, USA.

0148-0227/12/2011JG001874

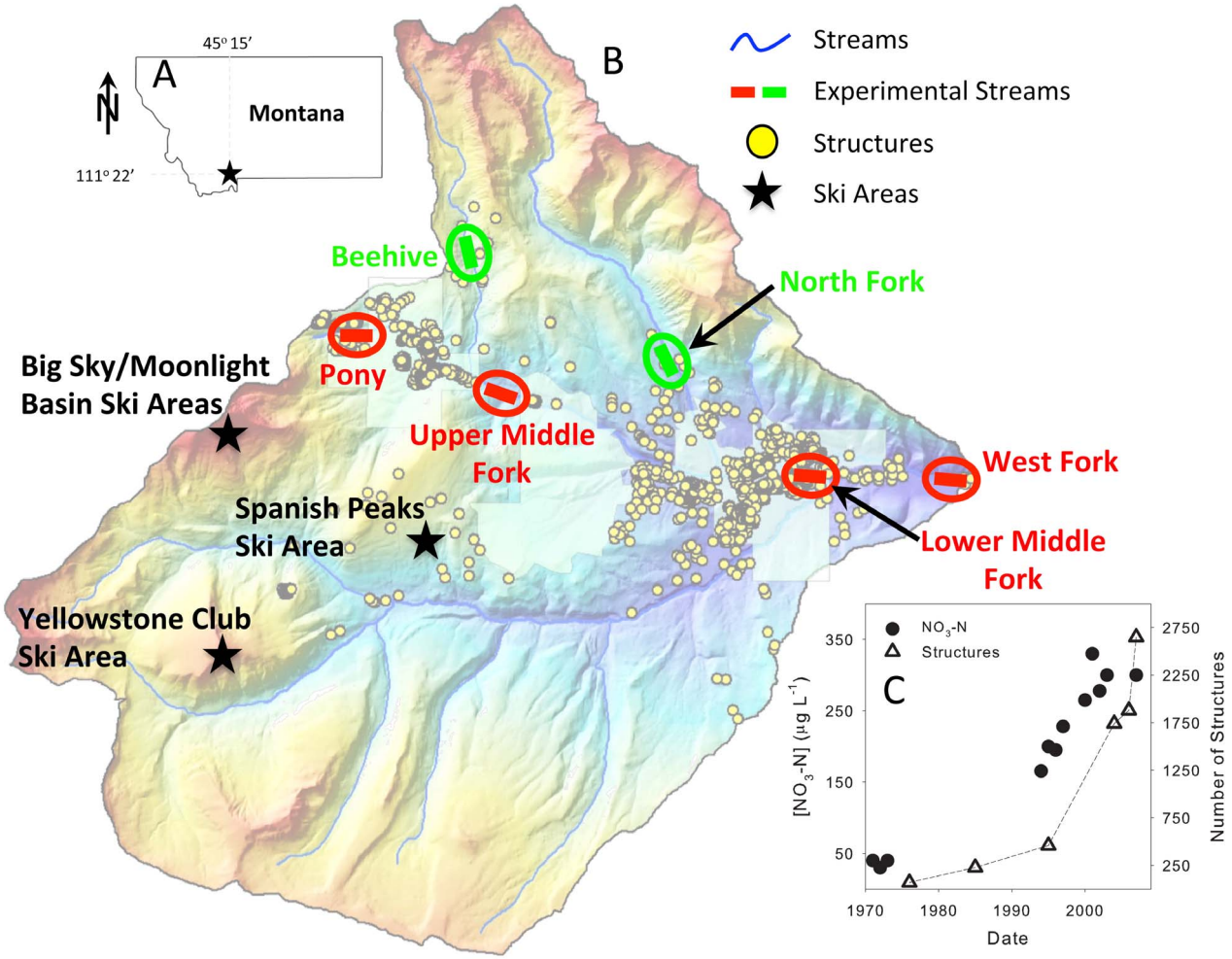

Figure 1. (a) Location of the West Fork Gallatin Watershed in southwestern Montana, USA; (b) detailed map of the 212 km^2 watershed with experimental streams and ski areas highlighted; and (c) time series of in-stream nitrate concentration and number of structures in the watershed since the 1970s.

N uptake and cycling across stream networks to assess the influence of increased nutrient loading and concentration on N retention capacities.

[4] Over recent decades, N loading in the West Fork Gallatin Watershed, Big Sky, Montana, has increased due to mountain resort development and consequent wastewater/septic inputs [*Gardner and McGlynn*, 2009]. We conducted multiple nutrient tracer experiments to quantify nitrate-nitrogen (NO_3-N) uptake dynamics across stream sizes and a development gradient to address the following: How do increases in watershed nutrient loading influence stream biogeochemical processes, and, specifically, how are nutrient uptake kinetics, nutrient spiraling, and nutrient retentive capacities influenced by land development and stream size?

2. Material and Methods

2.1. Study Area

[5] This research was conducted in the West Fork Gallatin Watershed, located in the Madison Mountain Range of Big Sky, Montana (Figure 1). Elevation in the West Fork Gallatin Watershed (212 km^2) ranges from 1800 to 3400 m with well-defined steep topography and shallow soils. In the valley bottoms, surficial geology is largely colluvium and glacial deposits while higher elevations are mainly comprised of sedimentary (e.g., gravel deposits) and metasedimentary (e.g., granitic gneiss) formations of various ages and metamorphosed volcanics of Archean age. From low to high elevations, precipitation ranges from less than 50 cm to more than 127 cm annually with the majority of precipitation falling as snow (Lone Mountain NRCS SNOTEL 590, 2707 m elevation). The growing season is short with 75–90 frost-free days (fewer frost-free days with increased elevation) from mid-June to mid-September (http://www.fs.fed.us/land/pubs/ecoregions/). In the higher elevations of the watershed, upland vegetation is comprised predominantly of Lodgepole pine (*Pinus contorta*), Blue spruce (*Picea pungens*), Engelmann spruce (*Picea engelmannii*), and Douglous fir (*Pseudotsuga menziesii*), with native grasses, willows (*Salix spp.*), and aspen (*Populus tremuloides*) groves in the riparian areas. In the lower elevations vegetation is predominantly native grasses, shrubs, and willows (*Salix spp.*). Streams in the watershed are low productivity (http://www.fs.fed.us/r1/gallatin/?page=resources/fisheries/

Table 1. Characteristics of the Six Experimental Streams and Dates When the Experiments Occurred

Site	Date	Stream Order	Watershed Area (km^2)	Discharge ($L\ s^{-1}$)	Stream Width (m)	Stream Temperature (°C)	Reach Length (m)	Stream Slope (%)	Number of Structures	Ash-Free Dry Mass ($mg\ cm^{-2}$)	Chlorophyll *a* ($\mu g\ cm^{-2}$)
Beehive	29 Jul 2008	2	5.7	137	2.7	7.0–12.4	588	1.7	4	0.50	0.25
Pony[a]	24 Aug 2007	1	0.9	6	1.1	4.8–8.7	625	8.8	125	0.41	0.56
North Fork	25–26 Jul 2007	2	22.8	146	3.1	8.7–12.5	1050	8.6	1	0.39	0.51
Upper Middle Fork[a]	1–2 Aug 2007	2	28.3	145	4.5	10.1–18.4	1043	3.7	650	0.82	1.17
Lower Middle Fork[a]	21–23 Aug 2007	3	83.4	199	7.0	9.2–13.8	1286	1.0	1690	1.30	2.20
West Fork[a]	25 Jul 2008	4	206.0	2439	10.6	8.1–15.3	1075	1.1	1880	1.28	1.89

[a]Streams draining developed subwatersheds.

streams), open canopy systems, and range in size from first to fourth order.

2.2. Experimental Design

[6] Our objective for the nutrient tracer experiments was to quantify NO_3-N uptake kinetics across stream sizes (first to fourth order) and along a development gradient in the West Fork Gallatin Watershed, Big Sky, Montana (Figure 1). Big Sky Resort was established in the early 1970s and since then land use/land cover change in the watershed has included the addition of three ski and golf resorts, construction of access roads, and residential development and associated septic and public sewer disposal systems. Since development began in the 1970s strong increases in both the number of structures in the watershed (mostly residential) and outlet stream water NO_3-N concentrations have occurred (Figure 1). Development has been focused in the upland locations of the watershed and has not encroached on near-stream or riparian areas or influenced vegetation in those locations [*Shoutis et al.*, 2010]. Additionally, there are currently no appreciable forestry, mining, or agricultural operations in the watershed.

[7] We conducted 17 stream tracer addition experiments on six streams across the West Fork Gallatin Watershed to quantify N uptake kinetics across stream sizes (first to fourth order) and along a development gradient (Figure 1). The six experimental streams were: Beehive, Pony, Upper Middle Fork, Lower Middle Fork, North Fork, and West Fork (listed in order of increasing watershed area, Figure 1). We paired four of the six streams in our analysis based on varying watershed area, stream discharge (Q), development, and stream water NO_3-N concentrations. Nutrient uptake kinetics and spiraling parameters were compared between streams draining undeveloped subwatersheds with lower [NO_3-N] and streams draining developed subwatersheds with higher in-stream [NO_3-N]. We selected comparison streams that were as similar as possible in all aspects except subwatershed development; however, some natural differences between the comparison streams did exist. While these stream pairs were not perfect, they were quite similar (except for development) and allowed us to assess the influence of development on in-stream NO_3-N uptake kinetics.

[8] Pony and Beehive were paired as the two small streams. Pony had greater development and higher stream water [NO_3-N] and Beehive had less development and lower stream water [NO_3-N] (Table 2, Figure 1). Upper Middle Fork and North Fork were paired as the two medium-sized streams. Upper Middle Fork had greater development and higher [NO_3-N] and North Fork had less development and lower [NO_3-N] (Table 2, Figure 1). Last, a developed-undeveloped pairing at the larger stream size was not possible because all of the larger streams near the watershed outlet, including Lower Middle Fork and West fork, are influenced by development (Tables 1 and 2 and Figure 1). For additional background water quality and watershed information, please see *Gardner and McGlynn* [2009] and *Gardner et al.* [2011]. We conducted nutrient addition experiments during July and August of 2007 and 2008 (Table 1).

2.3. Stream Discharge

[9] Immediately preceding the tracer addition experiments, we measured stream discharge at the downstream (base) and upstream (head) endpoints of each experimental reach using dilution gauging. Sodium chloride (NaCl) was fully dissolved in stream water and added as an instantaneous addition (i.e., slug) to the stream at a mixing length distance (20–100 m) upstream of the measurement location. Specific conductance was measured real-time at 2-s intervals at the downstream measurement location with Campbell Scientific (Logan, Utah) CS547A temperature and conductivity probes connected to Campbell Scientific CR1000 data loggers. We quantified the relationship between specific conductance and NaCl concentration ($r^2 = 0.999$, $p < 0.0001$) and from this relationship and breakthrough curve integration, we calculated Q [*Barbagelata*, 1928; *Covino et al.*, 2010b; *Day*, 1976; *Dingman*, 2002; *Kilpatrick and Cobb*, 1985].

2.4. Ash-Free Dry Mass and Chlorophyll *a*

[10] At each stream reach four rocks were selected and epilithic material was scrubbed from the rocks into a bucket of stream water. The resulting slurry was stored on ice and transported back to the laboratory where subsamples were filtered onto preashed 0.7 μm glass fiber filters (Whatman, Kent, UK). Filters for chlorophyll *a* analysis were frozen until acetone extraction, and chlorophyll *a* content was quantified using the fluorometric acidification method [*Steinman et al.*, 2006]. Separate filters for determination of ash-free dry mass were oven-dried at 60°C, weighed, combusted in a muffle furnace at 500°C for 2.5 h, and reweighed to ash-free dry mass.

2.5. Nutrient Tracer Experiments Using Constant-Rate Additions of Cl and NO_3-N

[11] Constant-rate additions were conducted on two of the six streams (Beehive and Lower Middle Fork). Stream reaches were 588 (Beehive) and 1286 m (Lower Middle Fork) in length (Table 1). We added a solution of fully dissolved NaCl (conservative tracer) and potassium nitrate (KNO_3, biologically active tracer) to the stream at a

constant-rate using a Fluid Metering pump (Fluid Metering Inc., Syosset, N. Y.). Specific conductance and temperature were measured real-time as described above. Specific conductance and temperature were measured at both the downstream and upstream endpoints of each stream reach at 10-s intervals during the constant-rate additions to guide sampling. Once the stream reached plateau based on observed specific conductance at the downstream endpoint, longitudinal samples were collected moving upstream from downstream. We sampled 10–12 longitudinal sampling sites evenly spaced along each reach, including sampling sites at both the downstream and upstream endpoints. In addition, each of these locations were sampled prior to the tracer additions to determine background concentrations (i.e., ambient N and Cl), and 20–40 measurements of stream width and depth were made to quantify general stream morphology. Stream water samples were also collected on 30 s to 10 min intervals at the furthest downstream sampling location during the rising and falling limbs to and from plateau concentrations. Frequency of sampling depended on the slope of the rising and falling limbs; samples were taken more frequently during times of greater rates of change in concentration.

[12] Samples were either filtered on site and kept in a cooler at ~4°C or kept in a cooler at ~4°C and filtered at the lab within 24 h of collection. All samples were filtered with Isopore Polycarbonate Membrane filters with a 0.4 μm pore size (Millipore, Billerica, Mass.). Filtered samples were then frozen in high-density polyethylene bottles until analysis. Each sample was analyzed for chloride (Cl^-) and nitrate (NO_3^-) by ion-exchange chromatography using a Metrohm ion chromatograph (IC) equipped with a 150 × 4.0 mm column (Metrohm Corp., Herisau, Switzerland). A 200 μl injection volume was used for low-level detection of anions. The analytical detection limits for NO_3^- and Cl^- were 5 and 2 μg l^{-1}, respectively. Standards prepared from reagent-grade salts were routinely checked against certified Alltech brand standards during IC sample analysis, and field and lab replicates were also analyzed. Accuracy of check standards and replicates was within 10%.

[13] Longitudinal stream samples collected during the plateau portion of constant-rate additions were used to calculate uptake length (S_w) [*Stream Solute Workshop*, 1990]. The slope of the linear regression between the natural log of background corrected NO_3-N:Cl of the longitudinal grab samples and distance downstream from the injection site is the plateau approach longitudinal uptake rate of added nutrient ($k_{w\text{-}add\text{-}plat}$), and plateau approach uptake length of added nutrient ($S_{w\text{-}add\text{-}plat}$) is

$$S_{w-add-plat} = -1/k_{w-add-plat}. \quad (1)$$

Plateau approach areal uptake rate ($U_{add\text{-}plat}$) and uptake velocity ($V_{f\text{-}add\text{-}plat}$) are

$$U_{add-plat} = \left(Q \times \left[NO_3 - N_{add-plat}\right]\right)/\left(w \times S_{w-add-plat}\right) \quad (2)$$

$$V_{f-add-plat} = U_{add-plat}/\left[NO_3 - N_{add-plat}\right], \quad (3)$$

where Q is stream discharge (L^3 T^{-1}), [NO_3-$N_{add\text{-}plat}$] is the geometric mean of background corrected NO_3-N concentrations of the longitudinal grab samples collected during plateau conditions (M L^{-3}), w is average wetted stream width (L), and $S_{w\text{-}add\text{-}plat}$ is uptake length of added nutrient during plateau (L).

2.6. TASCC Experiments Using Instantaneous Slug Additions of Cl and NO_3-N

[14] The six stream reaches where Tracer Additions for Spiraling Curve Characterization (TASCC) [*Covino et al.*, 2010a, 2010b] experiments occurred varied in length from 588 to 1286 m depending on stream size (i.e., streams with higher discharge had longer reach lengths, Table 1). We added a solution of NaCl (conservative tracer) and KNO_3 (biologically active tracer) to the stream as an instantaneous injection (i.e., slug). The masses of NaCl and KNO_3 added were dependent on stream [$NO_3 - N_{amb}$] and Q. Our goal was to raise NO_3-N levels one to two orders of magnitude above ambient conditions, and accordingly more nutrient tracer was added to streams with greater development and/or higher Q. Specific conductance and temperature were measured real-time using the equipment described previously. During TASCC experiments we measured specific conductance and temperature at both the downstream and upstream endpoints of the stream reach beginning before any influence of added tracer and continuing until after the stream had returned to background conditions (i.e., no influence of added tracers). Real-time specific conductance and temperature data were collected at a 10 s time step, and specific conductance data were used to guide sampling of the entire breakthrough curve. Stream water samples were collected on 30 s to 10 min intervals depending on the slope of the breakthrough curve; samples were taken more frequently during periods of more rapid changes in concentration. Stream water samples were filtered, handled, and analyzed as described above.

[15] We calculated added nutrient dynamic longitudinal uptake rates ($k_{w\text{-}add\text{-}dyn}$) for each grab sample by plotting the natural log of the NO_3-N:Cl ratio of injectate and each background corrected grab sample collected at the downstream endpoint against stream distance (Figure 2). The respective slopes of the lines from these data pairs are the $k_{w\text{-}add\text{-}dyn}$ values. The added nutrient dynamic uptake length ($S_{w\text{-}add\text{-}dyn}$) for each sample is the negative inverse of the $k_{w\text{-}add\text{-}dyn}$ values. Added nutrient dynamic areal uptake rates ($U_{add\text{-}dyn}$) and uptake velocities ($V_{f\text{-}add\text{-}dyn}$) are calculated as

$$U_{add-dyn} = \left(Q \times \left[NO_3 - N_{add-dyn}\right]\right)/\left(w \times S_{w-add-dyn}\right) \quad (4)$$

$$V_{f-add-dyn} = U_{add-dyn}/\left[NO_3 - N_{add-dyn}\right] \quad (5)$$

where Q is stream discharge (L^3 T^{-1}), [NO_3-$N_{add\text{-}dyn}$] is the geometric mean of observed (background corrected) and conservative NO_3-N concentration (M L^{-3}) of a grab sample, w is average wetted stream width (L) for the experimental reach, and $S_{w\text{-}add\text{-}dyn}$ is the dynamic uptake length of added nutrient (L). We define conservative NO_3-N as the amount of NO_3-N that would have arrived at a sampling site had NO_3-N traveled conservatively (i.e., no uptake, maximum that

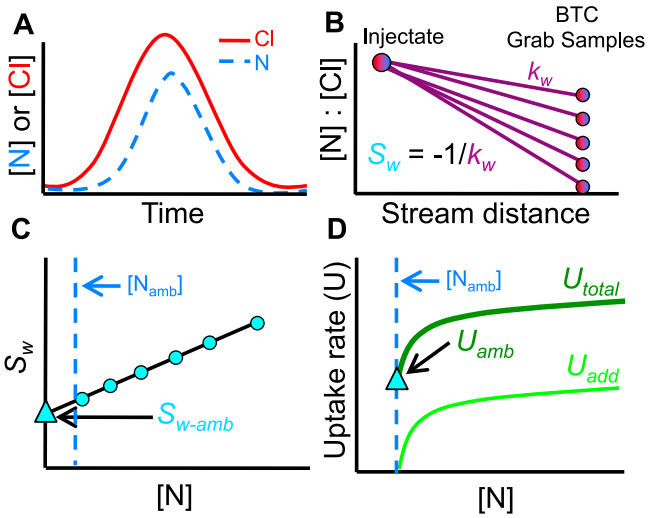

Figure 2. Schematic depiction of the Tracer Additions for Spiraling Curve Characterization (TASCC) approach (modified from *Covino et al.* [2010b]). (a) Sample the tracer breakthrough curves (BTCs), (b) calculate uptake lengths (S_w) for each grab sample, (c) utilize uptake lengths to extrapolate to ambient uptake length ($S_{w\text{-}amb}$), and (d) combine added nutrient (U_{add}) and ambient nutrient areal uptake rate (U_{amb}) to quantify total uptake (U_{tot}) and characterize the uptake kinetic curve.

could arrive), and calculate this as the product of observed Cl values (background corrected) and the NO_3-N:Cl ratio of the injectate.

[16] We determined ambient uptake lengths ($S_{w\text{-}amb}$) for each stream reach by regressing the $S_{w\text{-}add\text{-}dyn}$ values against in-stream concentration and extrapolating to ambient concentration to estimate $S_{w\text{-}amb}$ (Figure 2) [*Covino et al.*, 2010a; *Payn et al.*, 2005]. Ambient areal uptake rates (U_{amb}) and uptake velocities ($V_{f\text{-}amb}$) are calculated as

$$U_{amb} = Q \times [NO_3 - N_{amb}]/S_{w-amb} \times w \quad (6)$$

$$V_{f-amb} = U_{amb}/[NO_3 - N_{amb}] \quad (7)$$

where Q is stream discharge ($L^3\ T^{-1}$), [NO_3-N_{amb}] is the ambient stream NO_3-N concentration ($M\ L^{-3}$), w is average wetted stream width (L), and $S_{w\text{-}amb}$ is the ambient uptake length (L).

[17] Total nutrient uptake during an addition experiment is equal to the sum of ambient (i.e., background nutrient) and added nutrient uptake (Figure 2). We determined total nutrient uptake (U_{tot}) for both plateau and TASCC approaches [*Covino et al.*, 2010a] as the sum of ambient and added nutrient spiraling values:

$$U_{tot-plat} = U_{amb} + U_{add-plat} \quad (8)$$

$$U_{tot-dyn} = U_{amb} + U_{add-dyn} \quad (9)$$

where $U_{tot\text{-}plat}$ is the plateau approach total uptake ($M\ L^{-2}\ T^{-1}$), U_{amb} is the ambient uptake rate ($M\ L^{-2}\ T^{-1}$), $U_{add\text{-}plat}$ is the plateau approach uptake of added nutrient ($M\ L^{-2}\ T^{-1}$), $U_{tot\text{-}dyn}$ is the total dynamic areal uptake rate ($M\ L^{-2}\ T^{-1}$) for each grab sample, and $U_{add\text{-}dyn}$ is the dynamic areal uptake rate of added nutrient ($M\ L^{-2}\ T^{-1}$) for each grab sample. Total dynamic uptake velocity was calculated using

$$V_{f-tot-plat} = U_{tot-plat}/[NO_3 - N_{tot-plat}] \quad (10)$$

$$V_{f-tot-dyn} = U_{tot-dyn}/[NO_3 - N_{tot-dyn}] \quad (11)$$

where $V_{f\text{-}tot\text{-}plat}$ is the plateau approach total uptake velocity ($L\ T^{-1}$), [NO_3-$N_{tot\text{-}plat}$] is the geometric mean of total NO_3-N concentrations (i.e., not background corrected) ($M\ L^{-3}$) of the 12 samples collected along the stream reach during constant-rate plateau conditions, $V_{f\text{-}tot\text{-}dyn}$ is the total dynamic uptake velocity ($L\ T^{-1}$) for each grab sample from the BTC, and [NO_3-$N_{tot\text{-}dyn}$] is the geometric mean of the total observed and conservative NO_3-N concentration ($M\ L^{-3}$) in each grab sample:

$$[NO_3 - N_{tot-dyn}] = \sqrt{[NO_3 - N_{tot-obs}] \times ([NO_3 - N_{cons}] + [NO_3 - N_{amb}])} \quad (12)$$

where [NO_3-$N_{tot\text{-}obs}$] is the total observed NO_3-N concentration ($M\ L^{-3}$) in the samples collected throughout the BTC (note that this concentration is not background corrected).

3. Results

3.1. Physical and Biological Characteristics of the Experimental Streams

[18] During the tracer experiments discharge (Q) varied by three orders of magnitude and ambient nitrate-nitrogen (NO_3-N) concentration varied by one order of magnitude among the six experimental streams (Tables 1 and 2).

Table 2. Nutrient Concentrations and Nutrient Uptake Metrics for the Six Stream Reaches Where Tracer Experiments Occurred

Site	Ambient [NO_3-N] ($\mu g\ L^{-1}$)	Average Annual [NO_3-N] ($\mu g\ L^{-1}$)	$S_{w\text{-}amb}$ (m)	$V_{f\text{-}amb}$ (mm min^{-1})	U_{amb} ($\mu g\ m^{-2}\ min^{-1}$)	K_m ($\mu g\ L^{-1}$)	U_{max} ($\mu g\ m^{-2}\ min^{-1}$)
Beehive	2	21	1171	2.6	5	25	103
Pony[a]	68	202	625	0.5	33	458	201
North Fork	6	38	1265	2.4	14	88	209
Upper Middle Fork[a]	17	92	1020	1.9	32	1214	2041
Lower Middle Fork[a]	44	213	829	2.1	90	151	396
West Fork[a]	4	132	624	22.2	88	154	3594

[a]Streams draining developed subwatersheds.

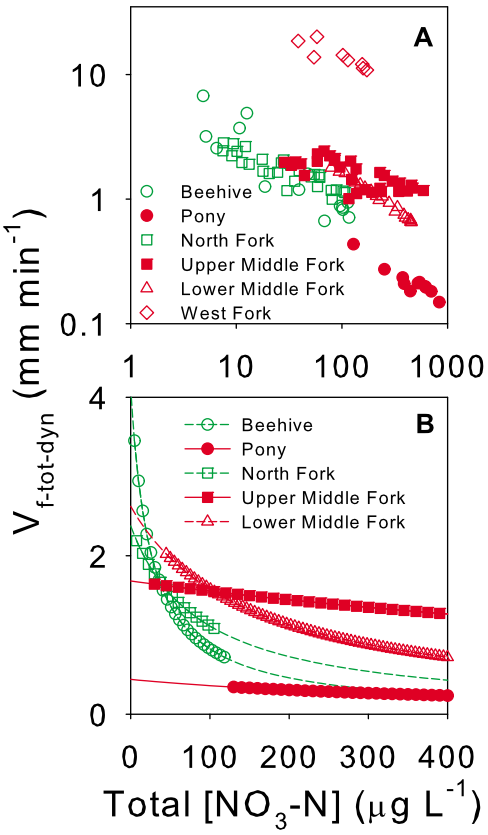

Figure 3. Dynamic uptake velocity ($V_{f\text{-}tot\text{-}dyn}$) as a function of total nitrate concentration showing (a) the experimental data from the six streams and (b) the Michaelis-Menten models derived from the experimental data for five of the streams (West Fork is excluded). The symbols in Figure 3b indicate the range of experimental data, and green indicates undeveloped and red indicates developed streams.

Ambient NO_3-N concentrations ranged from 2 to 68 ug L^{-1} and were higher in streams draining developed subwatersheds than in less developed systems (Table 2). Average annual NO_3-N concentrations ranged from 21 to 213 ug L^{-1} and again were greater in developed subwatersheds (Table 2). Epilithic ash-free dry mass, which is an indicator of biomass on the streambed, varied from 0.41 to 1.30 mg cm^{-2} and increased in the downstream direction (Table 1). Epilithic chlorophyll *a*, ranged between 0.25 and 2.20 μg cm^{-2}, increasing in the downstream direction, and was greater in developed as compared to less developed subwatersheds (Table 1).

3.2. Nutrient Uptake Kinetics Across the Experimental Streams

[19] From our measured uptake lengths (S_w) we calculated uptake velocities (V_f) and areal uptake rates (U) across the six experimental streams. Patterns and magnitudes of dynamic uptake velocities ($V_{f\text{-}tot\text{-}dyn}$) varied across the six streams (Figure 3). In the figures in this paper green symbols will indicate undeveloped and red symbols will indicate developed sites. Figure 3a displays $V_{f\text{-}tot\text{-}dyn}$ data in log-space and contains the West Fork values, which were much greater than $V_{f\text{-}tot\text{-}dyn}$ values for the remaining five streams. Figure 3b displays Michaelis-Menten (M-M) kinetic model fits to the $V_{f\text{-}tot\text{-}dyn}$ values [*Earl et al.*, 2006] for the five remaining streams and does not include the West Fork data. Across all streams $V_{f\text{-}tot\text{-}dyn}$ decreased with increasing [NO_3-$N_{tot\text{-}dyn}$], indicating decreased nutrient uptake efficiency at elevated concentration (Figure 3). In addition, the streams in undeveloped subwatersheds (Beehive and North Fork) had greater $V_{f\text{-}tot\text{-}dyn}$ relative to their respective comparison streams in developed subwatersheds (Pony and Upper Middle Fork) at low nutrient concentrations (Figure 3b). However, $V_{f\text{-}tot\text{-}dyn}$ values at elevated concentrations in undeveloped streams were comparable (see Beehive and Pony comparison) or even lower (see North Fork and Upper Middle Fork comparison) than $V_{f\text{-}tot\text{-}dyn}$ values for the developed streams (Figure 3b). Furthermore, the developed streams (Pony and Upper Middle Fork) had less of a decrease in $V_{f\text{-}tot\text{-}dyn}$ across the experimental concentration range than did the undeveloped sites (Figure 3b). Accordingly, the $V_{f\text{-}tot\text{-}dyn}$ curves at developed sites were relatively flat across the concentration ranges relative to undeveloped sites (Figure 3b).

[20] Uptake in all six streams followed hyperbolic M-M kinetics (Figure 4). Figure 4 displays the experimental data along with kinetic model fits (solid lines) and 95% confidence intervals (dashed lines) for the six streams. We determined uptake values at Beehive (Figure 4a) and Lower Middle Fork (Figure 4e) using both TASCC ($U_{tot\text{-}dyn}$) and plateau ($U_{tot\text{-}plat}$) approaches. $U_{tot\text{-}plat}$ values agreed well with $U_{tot\text{-}dyn}$ values and plotted along the dynamic uptake kinetic curves developed using the TASCC approach (Figures 4a and 4e). Maximum uptake values (U_{max}) among the sites ranged from 103 to 3594 (μg m^{-2} min^{-1}); Beehive (undeveloped) had the lowest value and West Fork (developed) the highest (Table 2 and Figure 4). In addition, half saturation constants (K_m) ranged from 25 to 1214 (μg L^{-1} NO_3-N); again Beehive had the lowest value but Upper Middle Fork (developed) had the highest K_m (Table 2 and Figure 4). U_{max} values generally increased with greater watershed area, and Upper Middle Fork and West Fork (both developed) had particularly high U_{max} values (Table 2 and Figure 4).

[21] We display M-M kinetic model fits for each of the comparison stream sets together in Figure 5 to aid in assessment of the influence of development intensity on nutrient uptake dynamics. For the Beehive–Pony stream pair, the less developed stream (Beehive) demonstrated a more rapid response to increased nutrient concentration (Figure 5a). This rapid response to nutrient addition is partially reflected in the lower K_m value at Beehive relative to Pony, indicating a steeper trajectory toward U_{max} (Table 2 and Figure 5a). However, both K_m and U_{max}, which define the shape of the uptake curve, need to be considered when assessing uptake dynamics. Although U at the undeveloped site (Beehive) responded more rapidly at lower concentrations, U_{max} at elevated concentrations was greater in the developed (Pony) subwatershed (Figure 5a). Conversely, for the North Fork–Upper Middle Fork stream pair, the developed stream (Upper Middle Fork) had consistently greater uptake compared to the undeveloped stream (North Fork) across the experimental concentration range (Figure 5b). The green and red shaded regions of Figures 5a and 5b indicate excess nutrient uptake at one of the streams relative to the

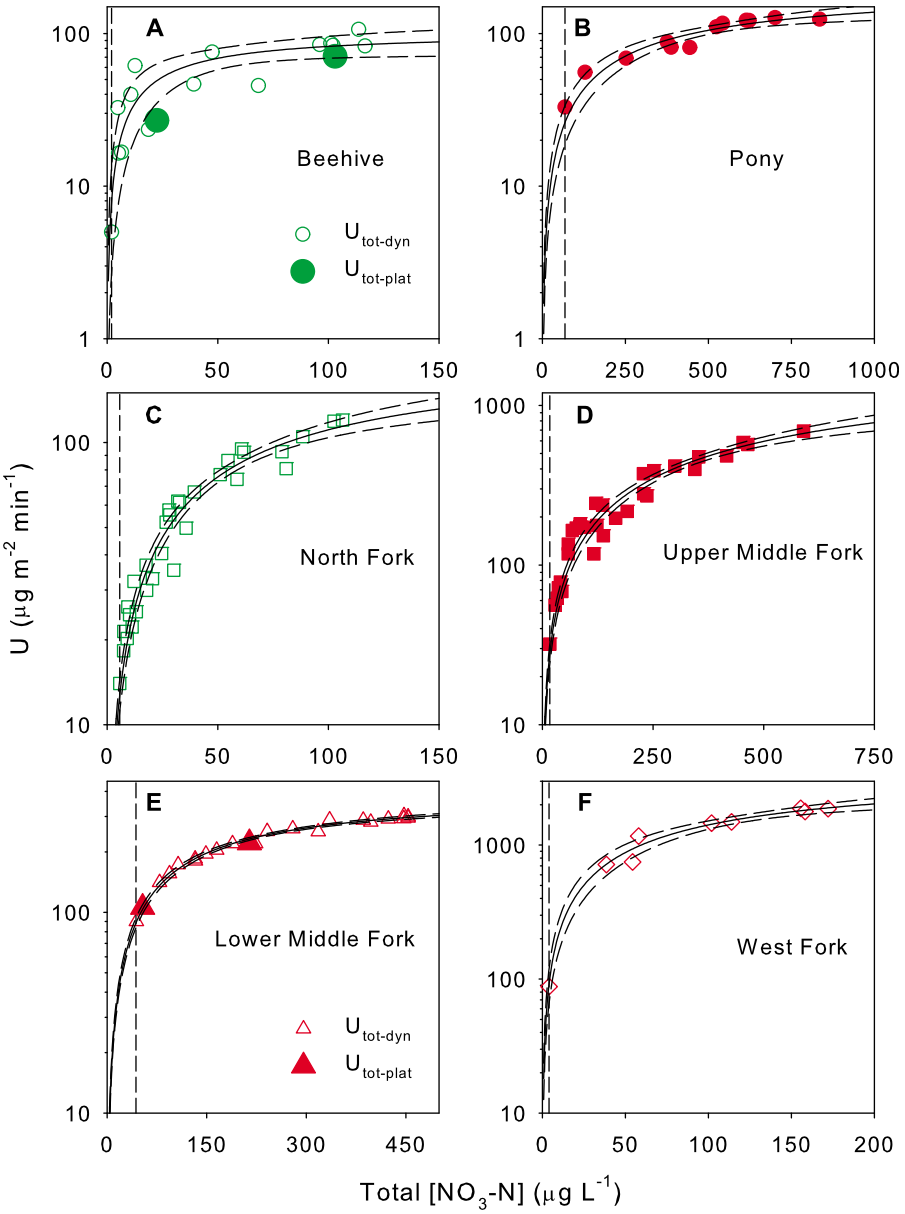

Figure 4. (a–f) Uptake curves as a function of nitrate concentration for the six streams. Symbols are experimental data, solid lines are the Michaelis-Menten model fits derived from the data, and dashed lines are the 95% confidence intervals. For Beehive (Figure 4a) and Lower Middle Fork (Figure 4e) we show both dynamic ($U_{tot-dyn}$) and plateau approach ($U_{tot-plat}$) experimental data. Green symbols indicate undeveloped and red indicate developed streams.

comparison stream. Areas that are shaded green represent greater nutrient uptake in the undeveloped site, and red regions indicate greater uptake in the developed site. For example, the green shaded region below concentrations of 400 μg L^{-1} NO_3-N on Figure 5a indicates higher nutrient retention capacity at Beehive (undeveloped) compared to Pony (developed).

[22] Beehive, North Fork, Upper Middle Fork, and Lower Middle Fork had similar nutrient uptake dynamics at concentrations less than 100 μg L^{-1} NO_3-N but diverged from one another at higher concentrations (Figure 6). Conversely, uptake at Pony (developed) was relatively low at concentrations below 200 μg L^{-1} NO_3-N, but was comparable to uptake at Beehive (undeveloped) at concentrations ~400 μg L^{-1} NO_3-N (Figure 6). Uptake at West Fork (developed) was far greater than uptake at all of the other streams across the entire range of NO_3-N concentrations (Figure 6).

[23] We used the M-M model fits for each stream to calculate uptake values at benchmark nutrient concentrations of 10, 50, 100, and 500 μg L^{-1} NO_3-N (Figure 7). At low concentrations U was greater at Beehive (undeveloped) than Pony (developed), however, U at Pony became larger at concentrations above 500 μg L^{-1} (Figure 7). For the North Fork–Upper Middle Fork comparison streams, U was greater at North Fork (undeveloped) at the 10 μg L^{-1}

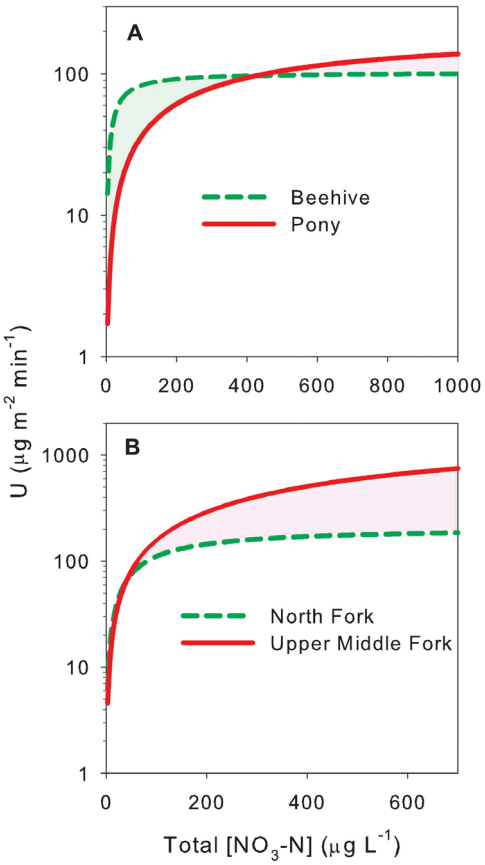

Figure 5. Comparison of uptake kinetic curves as a function of nitrate concentration for developed and undeveloped stream pairs. (a) Beehive represents the undeveloped and Pony represents the developed and (b) North Fork represents the undeveloped and Upper Middle Fork represents the developed stream. Again, green indicates undeveloped and red indicates developed streams and subwatersheds.

concentration, but U at Upper Middle Fork (developed) was greater at the remaining benchmark concentrations (Figure 7). Greatest U was consistently observed at West Fork, the largest stream located near the watershed outlet (Figure 7).

3.3. Relationships Between Uptake Kinetics and Stream Characteristics

[24] We present relationships between ambient uptake length ($S_{w\text{-}amb}$), ambient uptake velocity ($V_{f\text{-}amb}$), ambient areal uptake rate (U_{amb}), half-saturation constant (K_m), maximum uptake rate ($U_{\max}$), and ambient concentration (i.e., in-stream concentration at the time of the experiment) as well as average annual stream nutrient concentration (Figure 8). $S_{w\text{-}amb}$ varied from 624 to 1265 m across the six streams (Figure 8, Table 2). Interestingly, $S_{w\text{-}amb}$ values were shorter at developed streams relative to their comparison undeveloped streams (Table 2). Specifically, $S_{w\text{-}amb}$ was 1171 m at Beehive (undeveloped) and 625 m at Pony (developed) and 1265 m at North Fork (undeveloped) and 1020 at Upper Middle Fork (developed, Table 2). $S_{w\text{-}amb}$ decreased with both increased ambient [NO_3-N] and average annual [NO_3-N] (Figures 8a and 8b). This is counter to previous research that has shown longer S_w at elevated nutrient concentrations [*Hart et al.*, 1992; *Mulholland et al.*, 1990].

[25] Ambient uptake velocities ($V_{f\text{-}amb}$) were not significantly correlated to either ambient or average annual NO_3-N concentrations (Figures 8c and 8d). Beehive, North Fork, Upper Middle Fork, and Lower Middle Fork all had similar $V_{f\text{-}amb}$ values ranging from 1.9 to 2.6 mm min^{-1}, across an ambient [NO_3-N] range of 2 to 44 $\mu g\ L^{-1}$ and average annual [NO_3-N] from 21 to 213 $\mu g\ L^{-1}$ (Figures 8c and 8d). $V_{f\text{-}amb}$ was greater in the undeveloped (Beehive and North Fork) than their comparison streams (Pony and Upper Middle Fork, Table 2). Pony, the smallest stream both in terms of watershed area and Q (Table 1), had the highest [NO_3-N_{amb}] (68 $\mu g\ l^{-1}$), the second highest average annual [NO_3-N] (202 $\mu g\ l^{-1}$), and the lowest $V_{f\text{-}amb}$ (0.5 mm min^{-1}, Figures 8c and 8d, Table 2). Conversely, West Fork, the largest stream in terms of both watershed area and Q (Table 1), had the second lowest [NO_3-N_{amb}] (4 $\mu g\ l^{-1}$), the third highest average annual NO_3-N concentration (132 $\mu g\ l^{-1}$), and the highest $V_{f\text{-}amb}$ by an order of magnitude (22.2 mm min^{-1}, Figures 8c and 8d, Table 2).

[26] Ambient areal uptakes (U_{amb}), were not significantly correlated to either ambient or average annual NO_3-N concentrations (Figures 8e and 8f). U_{amb} ranged from 5 to 90 $\mu g\ m^{-2}\ min^{-1}$ and was lower in the undeveloped streams as compared to the developed streams (Figures 8e and 8f and Table 2). Highest U_{amb} was observed in the large streams: Lower Middle Fork (90 $\mu g\ m^{-2}\ min^{-1}$) and West Fork (88 $\mu g\ m^{-2}\ min^{-1}$) located near the watershed outlet (Table 2).

[27] Half-saturation constants (K_m), and maximum uptake rates ($U_{\max}$) were not significantly correlated to ambient or average annual NO_3-N concentration either (Figures 8g–8j). Both $U_{\max}$ and K_m were greater in developed than undeveloped streams (Table 2). Upper Middle Fork (developed) had

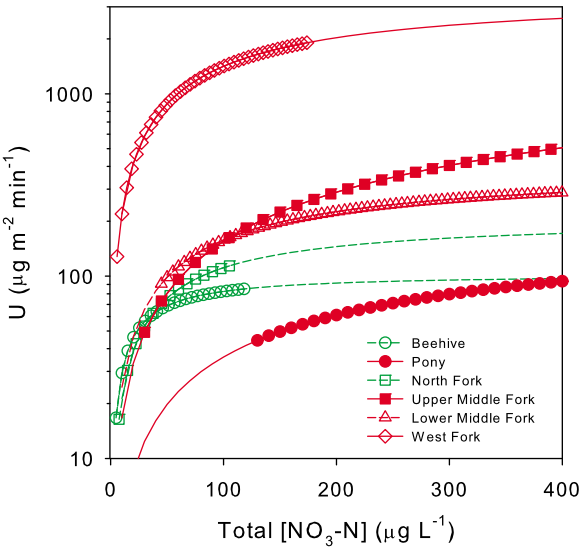

Figure 6. Michaelis-Menten model fits derived from the areal uptake data for the six streams; the symbols indicate the range of experimental data, and green indicates undeveloped and red indicates developed.

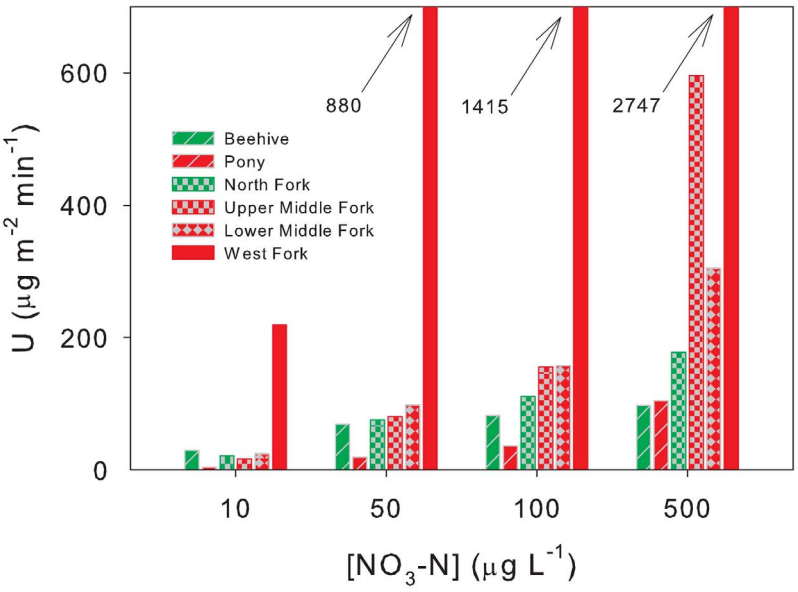

Figure 7. Areal uptake rates at benchmark concentrations across the six streams. These uptake values at benchmark concentrations were calculated using the Michaelis-Menten model fits derived from experimental data. Green indicates undeveloped stream sites and red indicates developed locations.

both the highest U_{max} and K_m, and Beehive (undeveloped) had the lowest U_{max} and K_m (Figure 8, Table 2).

[28] We assessed the relationships of U_{amb}, U_{max}, and K_m to watershed area, number of structures in the watershed (i.e., development intensity), epilithic ash-free dry mass, and epilithic chlorophyll *a* (Figures 9a–9l). We found statistically significant correlations between U_{amb} and number of structures, ash-free dry mass, and chlorophyll *a* and U_{max} and watershed area, ash-free dry mass, and chlorophyll *a* (Figure 9). Note that for the relationships between U_{max} and ash-free dry mass and chlorophyll *a*, there were only significant correlations when Lower Middle Fork was held out of the analysis (Figures 9h and 9k). Additionally, strong relationships were observed between U_{amb} and number of structures, and U_{amb} and chlorophyll *a* (both had $r^2 = 0.92$, Figures 9d and 9j), while ash-free dry mass explained 84% of the variance in U_{amb} between streams (Figure 9g). Number of structures, ash-free dry mass, and chlorophyll *a* were significant predictors of U_{amb} (Figures 9d, 9g, and 9j), however neither ambient nor average annual NO_3-N concentrations showed significant correlations with U_{amb} (Figure 8).

[29] We assessed the relationships of ash-free dry mass, and chlorophyll *a*, to watershed area, average annual NO_3-N concentration, and number of structures (Figures 10a–10f); as well as the relationship between average annual NO_3-N concentration and number of structures (Figure 10g). We observed significant correlations between ash-free dry mass and watershed area (Figure 10a), ash-free dry mass and average annual NO_3-N concentration (when Pony was held out, Figure 10c), and ash-free dry mass and number of structures (Figure 10e). Additionally, we observed significant correlations between chlorophyll *a* and average annual NO_3-N concentration (when Pony was held out, Figure 10d), and chlorophyll *a* and number of structures (Figure 10f). We observed strong relationships between ash-free dry mass and number of structures ($r^2 = 0.97$, Figure 10e), and chlorophyll *a* and number of structures ($r^2 = 0.94$, Figure 10f). Average annual NO_3-N concentration was only significantly correlated with either ash-free dry mass or chlorophyll *a* when Pony was not included in the analysis (Figures 10c and 10d).

4. Discussion

[30] *How do increases in watershed nutrient loading influence stream biogeochemical processes?* We quantified stream NO_3-N uptake kinetics and spiraling parameters along a development gradient across six streams draining subwatersheds of West Fork Gallatin Watershed to determine whether development and associated nutrient loading to streams impacted uptake kinetics. We compared developed and undeveloped streams of similar size and found differences in uptake kinetics between these streams. Uptake velocity (V_f) was greater at low concentrations in undeveloped streams compared to developed streams, indicating higher uptake efficiency in undeveloped streams at these concentrations (Figure 3). Indeed, $V_{f\text{-}amb}$ was greater in the undeveloped streams (Beehive and North Fork) than the developed (Pony and Upper Middle Fork) streams (Table 2). However, at elevated concentrations nutrient uptake efficiency indicated by V_f decreased sharply in undeveloped streams demonstrating loss of efficiency at high concentrations (Figure 3). Additionally, in the developed streams (Pony and Upper Middle Fork) we did not observe a sharp decrease in V_f at elevated NO_3-N concentration, and V_f remained fairly constant across the range of experimental concentrations in the developed streams (Figure 3). The developed streams receive greater annual N loads and the stability in V_f across the experimental concentration range could indicate stream adaptation to consistent nutrient sources. Specifically, that developed streams may not have a strong loss of efficiency (i.e., approach saturation) at

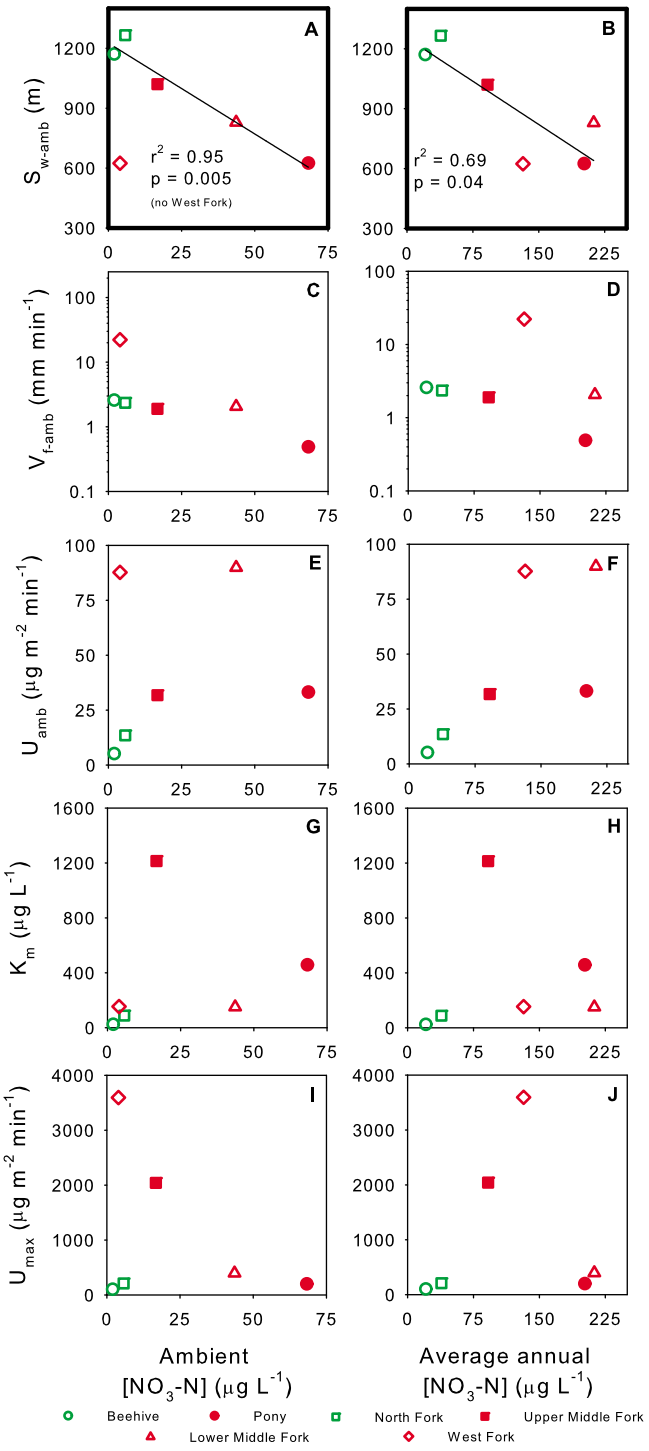

Figure 8. (a–j) Relationships between spiraling and kinetic metrics (ambient uptake length, $S_{w\text{-}amb}$; ambient uptake velocity, $V_{f\text{-}amb}$; ambient areal uptake rate, U_{amb}; half-saturation constant, K_m; and the maximum areal uptake rate, U_{max}) and ambient and average annual nitrate nitrogen concentration. Boldface indicates a significant correlation at the 0.05 level. Green symbols indicate undeveloped and red symbols indicate developed subwatersheds.

elevated N concentration compared to more pristine streams. None of the streams in this study indicated saturation with respect to N (i.e., NO_3-N addition resulted in increased uptake in all streams). Instead, it appears that increased loading in the developed streams has led to increased retention capacity across broad ranges of concentrations. This can be indicative of changes in biological community structure, including increased biomass and metabolic activity in response to chronic loading in the developed streams. However, continued or increased loading to these systems could eventually lead to conditions where demand is exceeded and N saturation occurs.

[31] Uptake dynamics followed M-M kinetics across all streams regardless of subwatershed development (Figures 4 and 6). However, U_{max}, K_m, and the shapes of the nutrient uptake curves varied among the six streams (Figures 4 and 6). Uptake responded rapidly to increasing concentration at Beehive (undeveloped), potentially indicating stronger N limitation in this stream as compared to Pony where uptake responded less abruptly to increases in concentration (Figures 5 and 6). This is evident in the steepness of the Beehive uptake curve at lower concentrations (Figure 5), and the smaller K_m for Beehive relative to Pony (Table 2). However, U_{max} was greater at Pony than Beehive (Table 2). This could indicate that initial response to nutrient loading/addition can be rapid in nutrient poor, undeveloped streams but that U_{max} and retentive capacity can be higher in developed, but not N saturated, streams with greater biomass. Greater loading can fertilize streams, increasing productivity and thereby increasing demand via a fertilization affect. The North Fork (undeveloped) and Upper Middle Fork (developed) comparison streams did not exhibit the same behavior as the Beehive–Pony streams. Specifically, uptake was consistently greater at Upper Middle Fork compared to North Fork across the experimental concentration range (Figure 5b). This could indicate a fertilization affect at Upper Middle Fork that has increased uptake across all concentrations due to greater biomass. Indeed, the red shaded region in Figure 5b indicates greater nutrient retention capacity at Upper Middle Fork compared to North Fork. Results from recent and ongoing whole watershed research in the West Fork Gallatin Watershed indicate that all of these systems are highly retentive of annual N loading [*Gardner and McGlynn*, 2009; *Gardner et al.*, 2011]. In fact, watershed retention of total dissolved nitrogen (TDN) ranged from 81% to 89% of total annual loads, indicating annual exports of only 11–19% [*Gardner and McGlynn*, 2009; *Gardner et al.*, 2011]. These results provide an annual watershed context for our research. Our findings indicate that these streams are not saturated, rather increased N loading as a result of development, has likely had a fertilization affect. This fertilization affect could lead to increased biomass and associated increases in nutrient retention capacity which could help maintain fractional export of annual N loading at low levels. Understanding the controls over watershed nutrient retention and assessing proximity to N saturation is important in light of the potentially deleterious impacts elevated export can have on downstream communities [e.g., *Rabalais et al.*, 2009].

[32] Ambient spiraling metrics across the streams were not consistently related to ambient or average annual nutrient concentration (Figure 8). We observed a significant negative

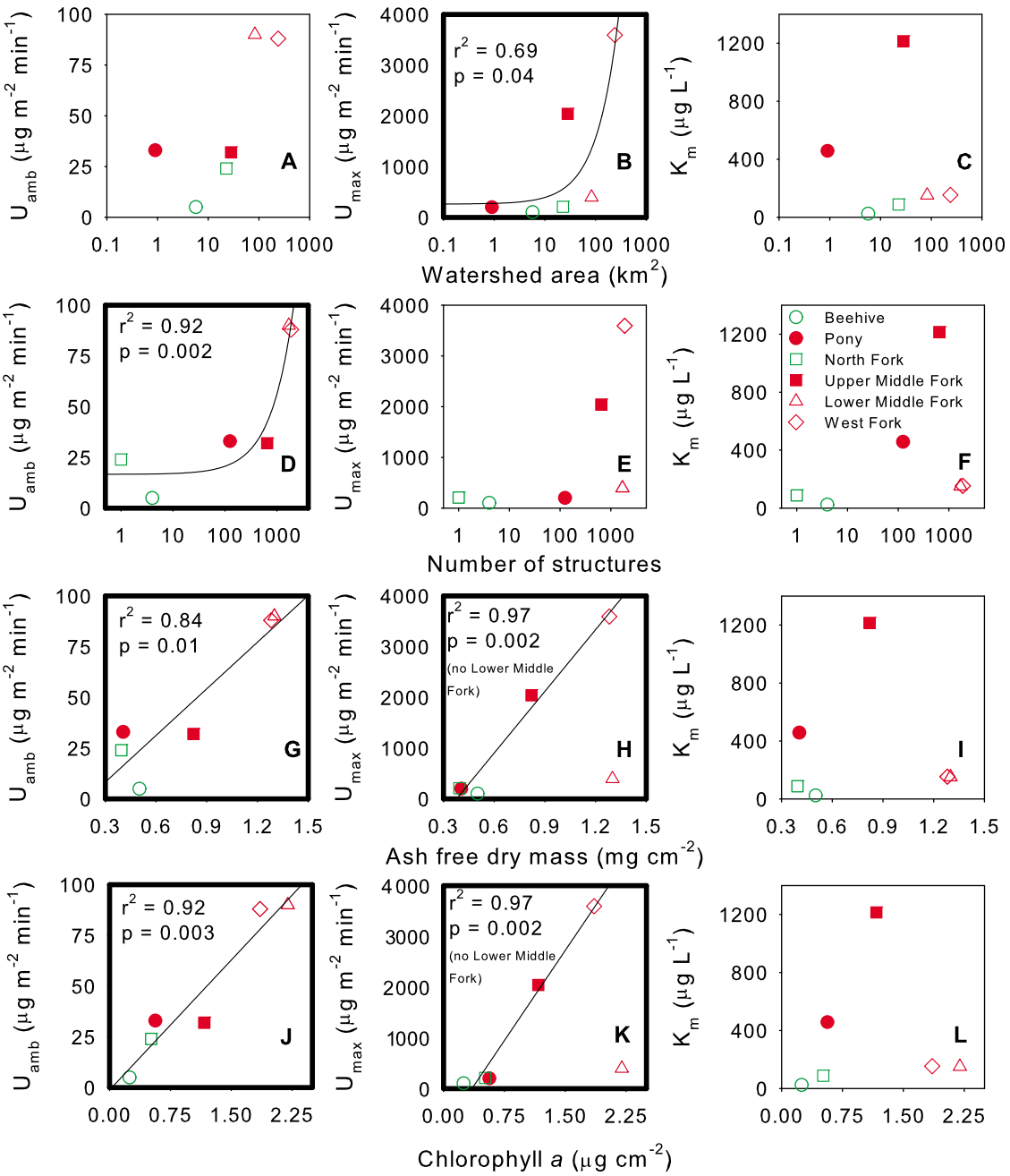

Figure 9. (a–l) Relationships of ambient areal uptake rate (U_{amb}), maximum areal uptake rate (U_{max}), and the half-saturation constant (K_m) to watershed area, number of structures in a subwatershed, ash-free dry mass, and chlorophyll *a*. Boldface indicates a significant correlation at the 0.05 level. Green symbols indicate undeveloped and red symbols indicate developed subwatersheds.

correlation between $S_{w\text{-}amb}$ and both ambient and average annual NO_3-N concentrations (Figures 8a and 8b). These relationships were counter to previously published research [e.g., *Hart et al.*, 1992; *Mulholland et al.*, 1990] and what is typically expected. Previous cross-system comparisons have observed increased S_w with increased nutrient concentration, although considerable variability exists in these regressions [*Earl et al.*, 2006]. Interstream comparisons are problematic partially because other variables (e.g., hydraulic conditions) in addition to nutrient concentration change from one system to the next. Furthermore, kinetic models are typically predicated on the assumption that biomass remains constant while only nutrient concentration varies, an assumption that is rarely if ever valid for interstream comparisons.

[33] Here, we did not observe significant correlations between $V_{f\text{-}amb}$ or U_{amb} and NO_3-N concentration (Figures 8c–8f). This is likely reflective of and highlights issues with interstream comparisons that have hampered attempts to develop global relationships between concentration and nutrient uptake across stream systems. Previous research has demonstrated decreased nutrient uptake efficiency, indicated by V_f, as well as hyperbolic increases in U with increasing

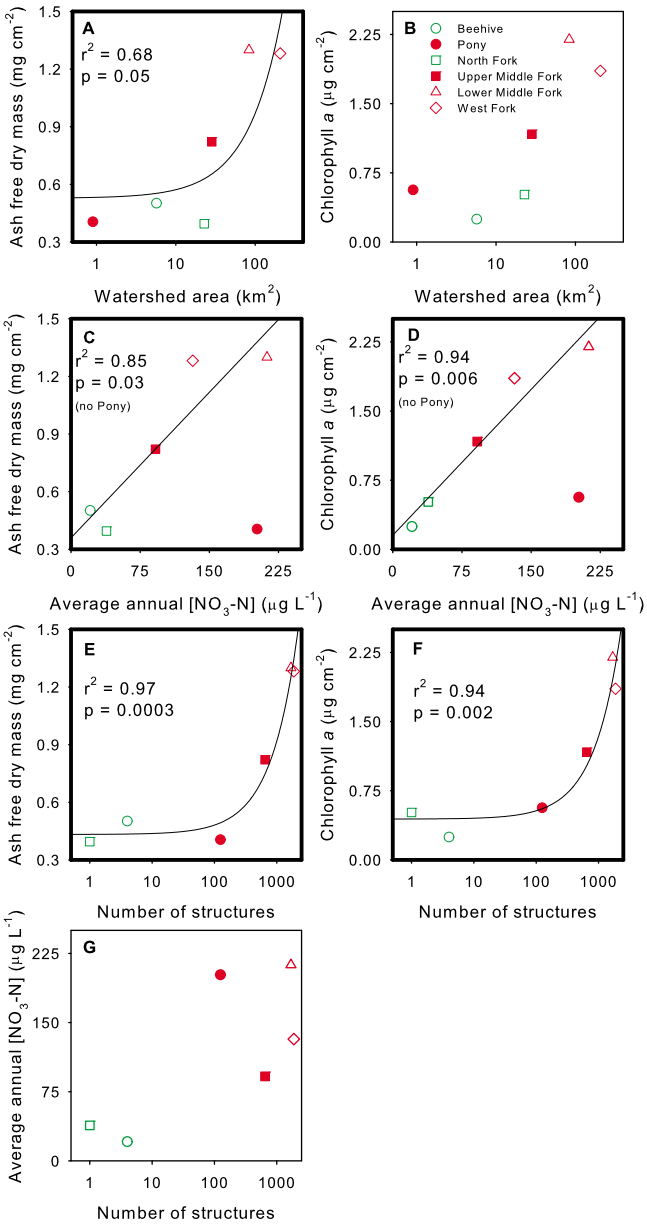

Figure 10. (a–f) Relationships of ash free dry mass and chlorophyll *a* to watershed area, average annual nitrogen, and number of structures, along with (g) average annual nitrate nitrogen and number of structures. Boldface indicates a significant correlation at the 0.05 level. Green symbols indicate undeveloped and red symbols indicate developed subwatersheds.

nutrient concentration in cross-system comparisons [*Dodds et al.*, 2002]. *Mulholland et al.* [2008] compiled nutrient uptake data from 72 streams, across eight regions, and several biomes and found a significant relationship between decreasing V_f and increasing nutrient concentration. However, here we found considerable variability in our assessment of the relationship between uptake metrics and concentration, which suggests that concentration (particularly ambient concentration) may not be a reliable indicator of nutrient uptake dynamics. This is partially due to the feedbacks between uptake and nutrient concentration. Specifically, as concentrations increase uptake will typically increase, in turn driving concentrations down. This feedback is continuous and can serve to buffer in stream concentrations.

[34] Additional watershed metrics were better indicators of ambient uptake and M-M kinetic model parameters than in-stream concentrations (Figure 9). For instance, we found significant relationships between U_{amb} and: the number of structures within a subwatershed, ash-free dry mass, and chlorophyll *a* (Figures 9d, 9g, and 9j). Furthermore, we found significant relationships between U_{max} and watershed area, ash-free dry mass (when Lower Middle Fork is not included), and chlorophyll *a* (when Lower Middle Fork is not included, Figures 9b, 9h, and 9k). These analyses suggest increased development and consequently elevated nutrient loading can influence stream biomass, productivity, and nutrient uptake and retention dynamics. The increase in ash-free dry mass co-occurs with increasing watershed area (see Figure 10a); however, the number of structures was a stronger predictor of ash-free dry mass than area (see Figure 10e). In addition, the number of structures in a subwatershed was also strongly correlated to chlorophyll *a* (see Figure 10f). These relationships suggest that land use/land cover change in the form of residential development can have significant impacts on freshwater ecology and stream biological communities as shown with biomass and nutrient cycling changes. This has important implications for ecosystem function and water quality alteration. Here, the streams did not exhibit saturation with respect to N but we did observe a fertilization affect. Development has led to increased nutrient loading to adjacent streams, resulting in increased biomass (ash-free dry mass), increased primary productivity (chlorophyll *a*), and enhanced N retentive capacity. This increased retentive capacity responds to and could partially compensate for elevated loading thereby helping maintain nutrient export at relatively low levels [*Gardner et al.*, 2011]. Increased loading and subsequent increases in biomass can in turn drive down in-stream nutrient concentrations over short time scales. These dynamics are partially responsible for similar ambient nutrient concentrations in spite of strong differences in loading between streams. For instance, Beehive (undeveloped) and West Fork (developed) have large differences in nutrient loading but similar ambient nutrient concentrations, potentially due to the strong uptake at West Fork, which can cause short-term decreases in concentrations. However, it is unclear at what point saturation or near saturation conditions with respect to N could or will occur. If N saturation is realized, large increases in annual N export would be expected. Given obvious concerns associated with downstream loading [e.g., *Rabalais et al.*, 2009], careful assessment of aquatic ecosystem proximity to saturation should be considered when addressing elevated loading from land use/land cover change including development, agricultural practices, or disturbance.

5. Summary

[35] Substantial increases in development in the West Fork Gallatin Watershed have occurred since the early 1970s. As a consequence, in-stream nutrient concentrations have also increased. While nitrate-nitrogen (NO_3-N)

retention and uptake dynamics were influenced by these elevated concentrations, streams do not yet appear to be experiencing NO_3-N saturation. We observed that stream uptake kinetics and spiraling parameters varied across streams of different development intensity and scale. Our results indicated that ambient uptake efficiencies (V_f), in undeveloped streams were higher and decreased more rapidly in response to increases in concentration than streams in more developed subwatersheds. We found that half-saturation (K_m) values were greater in undeveloped streams, while maximum uptake rates ($U_{\max}$) were larger in developed systems. This suggests that land use/land cover change and associated nutrient loading can have substantial influences on in-stream nutrient uptake dynamics. We observed strong relationships between the number of structures in a subwatershed and in-stream ambient uptake (U_{amb}), epilithic ash-free dry mass, and epilithic chlorophyll *a*. However, we did not observe statistically significant relationships between kinetic parameters and ambient or average annual [NO_3-N], suggesting that in-stream concentrations could be poor indicators of uptake dynamics. Conversely, the strong relationships between the number of structures in a subwatershed and biological community metrics such as ash-free dry mass and chlorophyll *a* suggest land use/land cover change can affect stream ecosystem structure and productivity. While the streams we examined did not exhibit N saturation behavior, they were affected by development and associated increases in nutrient loading. Increased N retention capacities have partially compensated for elevated loading and could help maintain export at low levels. However, if watershed loading continues to increase, N saturation and large export to downstream communities is possible. Improved understanding of the watershed dynamics that control nutrient export across scales and development intensities, along with indicators of biological community nutrient status are requisite for mitigation and protection of aquatic ecosystems.

[36] **Acknowledgments.** Financial support was provided by National Science Foundation (NSF) Ecosystems DEB-0519264, NSF EPSCoR Montana Institute on Ecosystems Fellowship awarded to Covino, an Environmental Protection Agency (EPA) STAR Fellowship awarded to Covino, EPA STAR grant R832449, EPA 319 funds administered by the Montana Department of Environmental Quality, and the USGS 104(b) grant program administered by the Montana Water Center. We thank Leslie Piper for ash-free dry mass and chlorophyll a data, Galena Ackerman and John Mallard for laboratory analysis, and Tricia Jenkins for help collecting field samples. We thank the Big Sky community for allowing access to sampling sites.

References

Barbagelata, A. (1928), Chemical-electrical measurement of water, *Proc. Am. Soc. Civ. Eng.*, *54*, 789–802.

Biggs, T. W., T. Dunne, and L. A. Martinelli (2004), Natural controls and human impacts on stream nutrient concentrations in a deforested region of the Brazilian Amazon basin, *Biogeochemistry*, *68*(2), 227–257, doi:10.1023/B:BIOG.0000025744.78309.2e.

Covino, T. P., B. L. McGlynn, and R. A. McNamara (2010a), Tracer Additions for Spiraling Curve Characterization (TASCC): Quantifying stream nutrient uptake kinetics from ambient to saturation, *Limnol. Oceanogr. Methods*, *8*, 484–498, doi:10.4319/lom.2010.8.484.

Covino, T. P., B. L. McGlynn, and M. A. Baker (2010b), Separating physical and biological nutrient retention and quantifying uptake kinetics from ambient to saturation in successive mountain stream reaches, *J. Geophys. Res.*, *115*, G04010, doi:10.1029/2009JG001263.

Day, T. J. (1976), Precision of salt dilution gauging, *J. Hydrol.*, *31*(3-4), 293–306, doi:10.1016/0022-1694(76)90130-X.

Dingman, S. L. (2002), Stream-gauging methods for short-term studies, in *Physical Hydrology*, edited by S. L. Dingman, pp. 613–615, Prentice Hall, Upper Saddle River, N. J.

Dodds, W. K., et al. (2002), N uptake as a function of concentration in streams, *J. N. Am. Benthol. Soc.*, *21*(2), 206–220, doi:10.2307/1468410.

Earl, S. R., H. M. Valett, and J. R. Webster (2006), Nitrogen saturation in stream ecosystems, *Ecology*, *87*(12), 3140–3151, doi:10.1890/0012-9658(2006)87[3140:NSISE]2.0.CO;2.

Ensign, S. H., and M. W. Doyle (2006), Nutrient spiraling in streams and river networks, *J. Geophys. Res.*, *111*, G04009, doi:10.1029/2005JG000114.

Gardner, K. K., and B. L. McGlynn (2009), Seasonality in spatial variability and influence of land use/land cover and watershed characteristics on stream water nitrate concentrations in a developing watershed in the Rocky Mountain West, *Water Resour. Res.*, *45*, W08411, doi:10.1029/2008WR007029.

Gardner, K. K., B. L. McGlynn, and L. A. Marshall (2011), Quantifying watershed sensitivity to spatially variable N loading and the relative importance of watershed N retention mechanisms, *Water Resour. Res.*, *47*, W08524, doi:10.1029/2010WR009738.

Grimm, N. B., and S. G. Fisher (1986), Nitrogen limitation in a Sonoran desert stream, *J. N. Am. Benthol. Soc.*, *5*(1), 2–15, doi:10.2307/1467743.

Hart, B. T., P. Freeman, and I. D. McKelvie (1992), Whole-stream phosphorus release studies: Variation in uptake length with initial phosphorus concentration, *Hydrobiologia*, *235-236*, 573–584, doi:10.1007/BF00026245.

Kilpatrick, F. A., and E. D. Cobb (1985), Measurement of discharge using tracers, in *Applications of Hydraulics*, *Tech. Water-Resour. Invest. Rep. Ser.*, vol. 3, chap. A16, pp. 1–52, U. S. Geol. Surv., Reston, Va.

Mueller, D. K., and N. E. Spahr (2006), *Nutrients in Streams and Rivers Across the Nation—1992–2001*, 51 pp., U. S. Geol. Surv., Reston, Va.

Mulholland, P. J., and J. R. Webster (2010), Nutrient dynamics in streams and the role of J-NABS, *J. N. Am. Benthol. Soc.*, *29*(1), 100–117.

Mulholland, P. J., A. D. Steinman, and J. W. Elwood (1990), Measurement of phosphorus uptake length in streams: Comparison of radiotracer and stable PO_4 releases, *Can. J. Fish. Aquat. Sci.*, *47*(12), 2351–2357, doi:10.1139/f90-261.

Mulholland, P. J., et al. (2008), Stream denitrification across biomes and its response to anthropogenic nitrate loading, *Nature*, *452*(7184), 202–205, doi:10.1038/nature06686.

Payn, R. A., J. R. Webster, P. J. Mulholland, H. M. Valett, and W. K. Dodds (2005), Estimation of stream nutrient uptake from nutrient addition experiments, *Limnol. Oceanogr. Methods*, *3*, 174–182, doi:10.4319/lom.2005.3.174.

Peterson, B. J., et al. (2001), Control of nitrogen export from watersheds by headwater streams, *Science*, *292*(5514), 86–90, doi:10.1126/science.1056874.

Rabalais, N. N., R. E. Turner, R. J. Diaz, and D. Justic (2009), Global change and eutrophication of coastal waters, *ICES J. Mar. Sci.*, *66*(7), 1528–1537, doi:10.1093/icesjms/fsp047.

Rabalais, N. N., R. J. Diaz, L. A. Levin, R. E. Turner, D. Gilbert, and J. Zhang (2010), Dynamics and distribution of natural and human-caused hypoxia, *Biogeosciences*, *7*(2), 585–619, doi:10.5194/bg-7-585-2010.

Shoutis, L., D. T. Patten, and B. McGlynn (2010), Terrain-based predictive modeling of Riparian vegetation in a northern Rocky Mountain watershed, *Wetlands*, *30*(3), 621–633, doi:10.1007/s13157-010-0047-5.

Steinman, A. D., G. A. Lamberti, and P. R. Leavitt (2006), Biomass and pigments of benthic algae, in *Methods in Stream Ecology*, edited by F. R. Hauer and G. A. Lamberti, pp. 357–379, Academic, San Diego, Calif.

Vitousek, P. M., and R. W. Howarth (1991), Nitrogen limitation on land and in the sea: How can it occur?, *Biogeochemistry*, *13*, 87–115, doi:10.1007/BF00002772.

Whitehead, P. G., P. J. Johnes, and D. Butterfield (2002), Steady state and dynamic modelling of nitrogen in the River Kennet: Impacts of land use change since the 1930s, *Sci. Total Environ.*, *282-283*, 417–434, doi:10.1016/S0048-9697(01)00927-5.

Workshop, S. S. (1990), Concepts and methods for assessing solute dynamics in stream ecosystems, *J. N. Am. Benthol. Soc.*, *9*(2), 95–119, doi:10.2307/1467445.

T. Covino, B. McGlynn, and R. McNamara, Department of Land Resources and Environmental Sciences, Montana State University, 334 Leon Johnson Hall, Bozeman, MT 59717, USA. (tpcovino@gmail.com)